On the factors governing the abundance of oxalic acid in tropospheric aerosol particles

LEIBNIZ-INSTITUT FÜR TROPOSPHÄRENFORSCHUNG

Dominik van Pinxteren, Christian Neusüß[a], Erika Brüggemann, Thomas Gnauk, Konrad Müller, Hartmut Herrmann

Leibniz – Institute for Tropospheric Research, Permoserstraße 15, 04318 Leipzig, Germany

[a] Hochschule Aalen, Beethovenstr. 1, 73430 Aalen, Germany

Motivation

- Oxalic acid one is of the most abundant single organic species in particles (Saxena and Hildemann, 2000)
- Secondary sources
- Different formation pathways in state-of-the-art multiphase models (Fig. 1):
  - anthropogenic: starting from aromatic VOCs (e.g. Ervens et al., 2003)
  - biogenic: starting from isoprene and monoterpenes (e.g. Lim et al., 2005)
  - marine: starting e.g. from ethene (Warneck, 2003)
- Can field measurements reveal the type of dominant precursors?

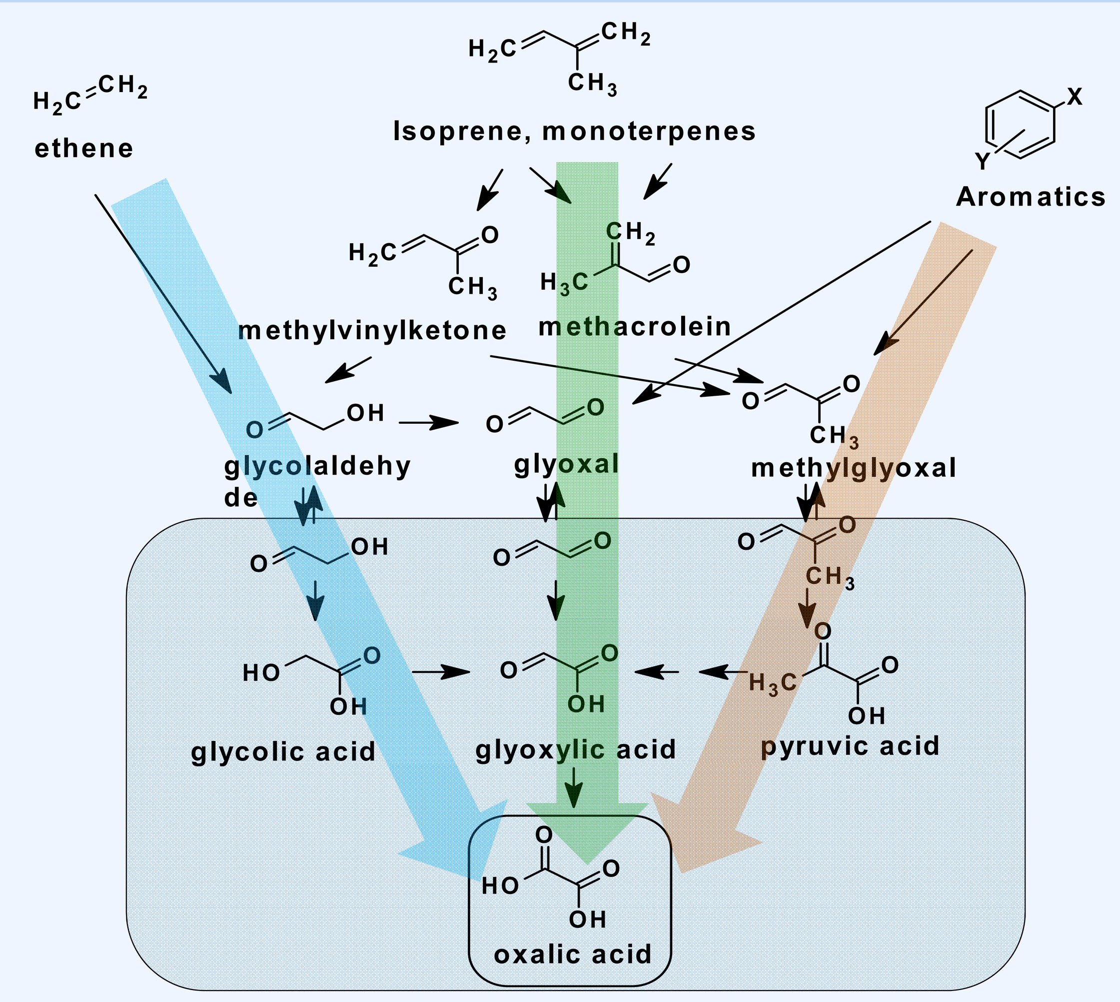

Fig. 1: Some simplified known pathways of oxalic acid production

Sampling and Analysis

- 144 5-stage Berner samples were taken at 6 different locations in Europe (Fig. 2 and Table 1)
- 1 coastal, 3 rural and 2 urban background sites (Table 1)
- Samples were analyzed for oxalic acid by capillary electrophoresis after aqueous extraction (Neusüß et al., 2000)

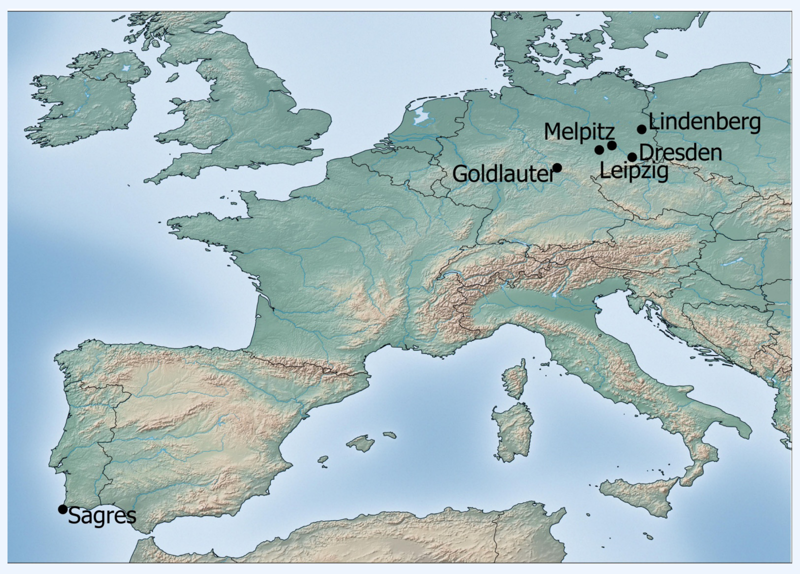

Fig. 2: Map of sampling sites

Table 1: Information on different campaigns

Site	Season	Time of sampling	Type of site	No. samples	Hrs/sample
Sagres	Summer	Jun - Jul 1997	Coastal	49	4-46
Melpitz	Fall	Oct - Nov 1997	Rural	20	8-27
Lindenberg	Summer	Jul - Aug 1998	Rural	23	7-23
Goldlauter	Fall	Oct 2001 and Oct 2002	Rural/Forest	10	5-16
Leipzig	Summer and Winter	Jul 2003 - Aug 2005	Urban Background	30	24
Dresden	Year-round	Sep 2003 - Aug 2004	Urban Background	12	24

Back trajectory and land cover analysis

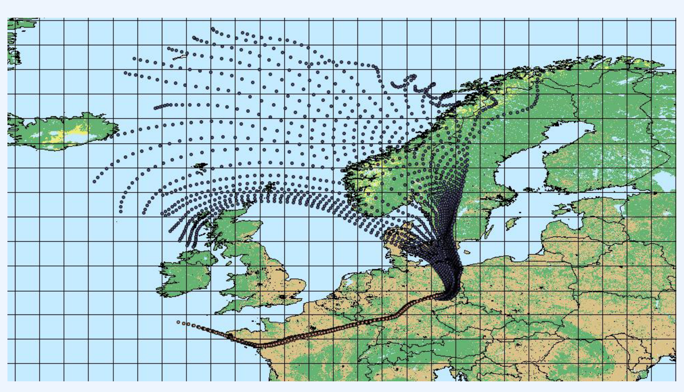

Fig. 3: Modified GLC2000 land cover map with 2x2 grid and example back trajectories

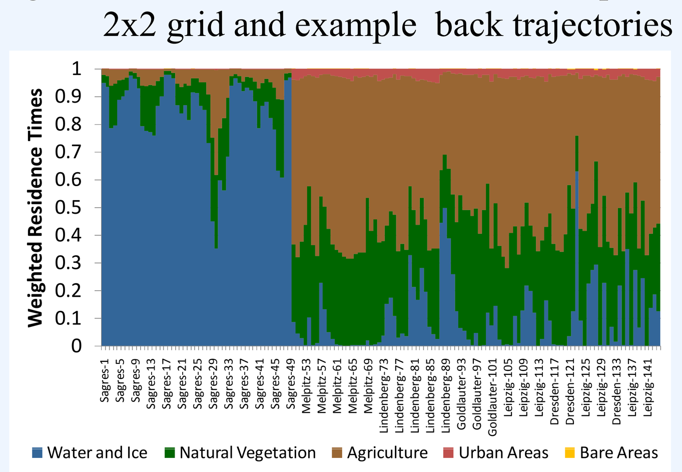

Fig. 4: Weighted residence times for all samples

- 96 h backward trajectories were calculated with HYSPLIT (Draxler and Rolph, 2010)
- 1 trajectory per hour during sampling interval, starting height 10 m, FNL dataset
- Land cover data was taken from the Global Lanc Cover 2000 database (GLC2000)
- Land cover data was remapped to 5 classes: Water and Ice, Natural Vegetation, Agriculture, Urban Areas, Bare Areas
- A 2° x 2° grid was superimposed and area fraction F_{mnk} for each grid cell (m,n) and each land cover class k was calculated
- Index $X_{ik}(S)$ was calculated as a proxy for the age-weighted residence time (WRT) above land cover class k of back trajectory i within a sampling interval S:

$$X_{ik} = \frac{1}{\sum_{j=1}^{J} w_j} \sum_{j=1}^{J} w_j F_{mnk}$$

where j = 0,1,...,J: hourly endpoints of trajectory (here J = 96)

and $w_j = 1 - j/J$: linear weighting function, reflecting the decreasing influence of "later" trajectory points

- Index $X_k(S)$ was derived as proxy for the WRT above land cover class k for sample S by calculating the arithmetic mean of all X_{ik} within one sample S
- Average length of trajectories, meteorology along trajectory, mixing layer depth at sampling site was calculated from Hysplit model output for each sample

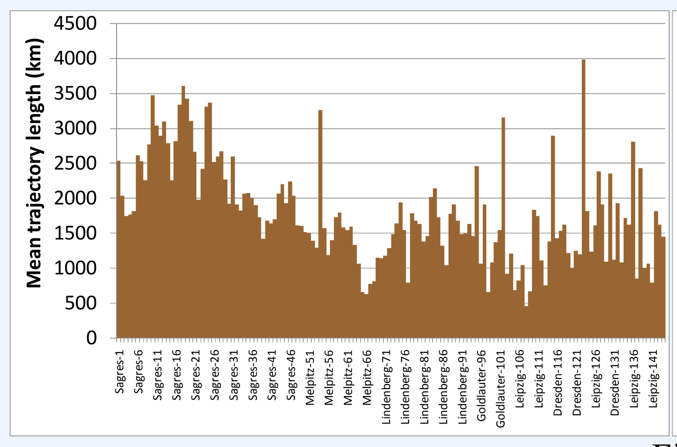

Fig. 5: Average back trajectory length for all samples

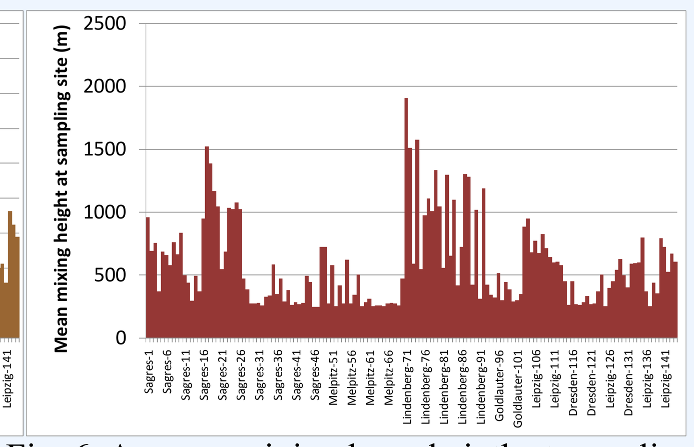

Fig. 6: Average mixing layer heigth at sampling site from Hysplit output for all samples

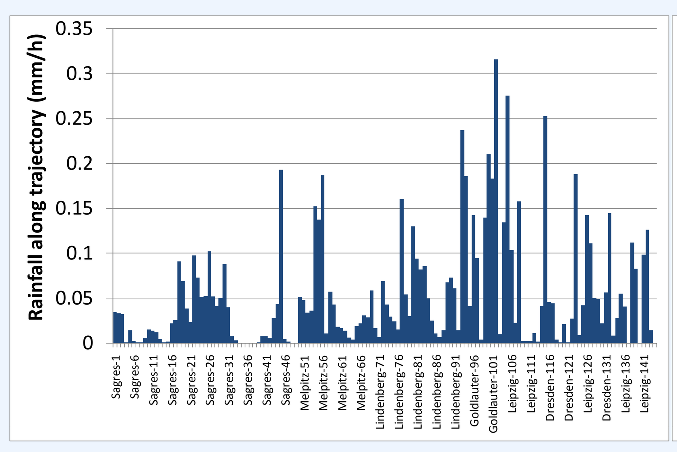

Fig. 7: Sum of rainfall along back trajectory for all samples

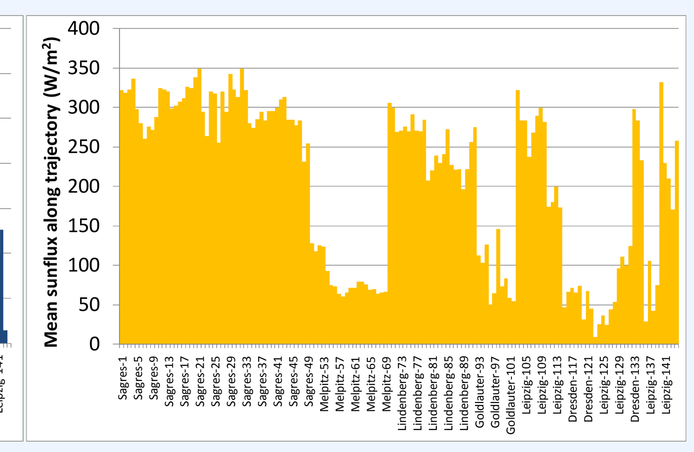

Fig. 8: Average sunflux along back trajectory for all samples

Concentrations and size distributions

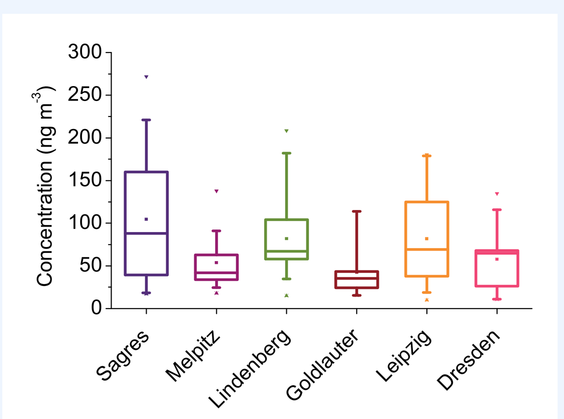

Fig. 9: Box plots of oxalic acid PM_{10} concentrations at different sites

- PM_{10} oxalic acid ranges from 10 to 272 ng m^{-3}
- Campaigns including summertime sampling show higher mean concentrations (Fig. 9)
- Concentration spread is highest at coastal site, even though only summertime sampling (Fig. 9)

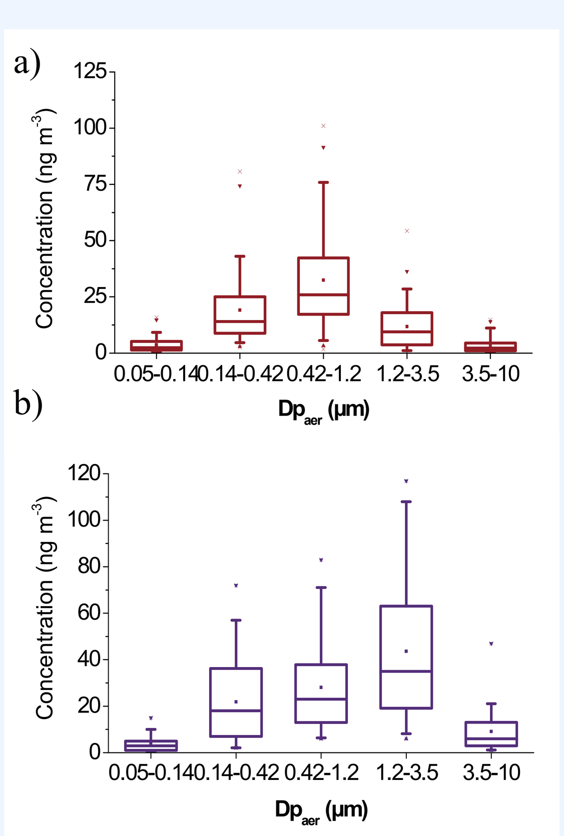

Fig. 10: Box plots of oxalic acid concentrations in impactor size ranges for a) continenal site and b) coastal site

- Size-resolved data show typical accumulation mode maximum at continental sites (Fig. 10a)
- At coastal site there is clear influence of oxalate containing sea salt particles at Dp_{aer} = 1.2 – 3.5 µm (Fig. 10b)
- The concentrations in smallest (Dp_{aer} = 0.05-0.14 µm) and largest (Dp_{aer} = 3.5-10 µm) particles are very low at both sites (Fig. 10a and b)

Back trajectory and land cover results

- Clearly different air mass types at coastal vs. cont. sites (Fig. 11)

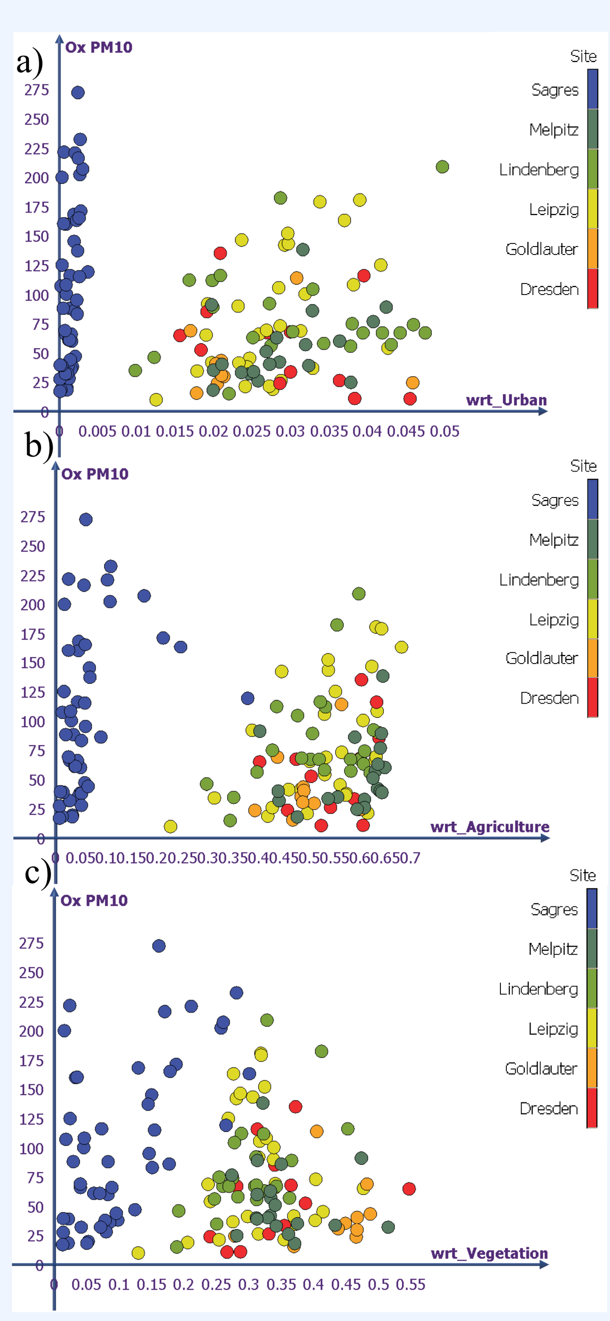

Fig. 11: PM_{10} oxalic acid concentration (in ng m^{-3}) vs. a) WRT above urban areas, b) WRT above agricultural areas, c) above natural vegetation at different sampling sites

- Trend of high oxalate conc. at high WRT above urban and agricultural areas (anthropogenic influence), but poor correlation (Fig. 12)
- Trend of high oxalate conc. when both sunflux and anthrop. influence are high in coastal and continental regime (Fig. 12)

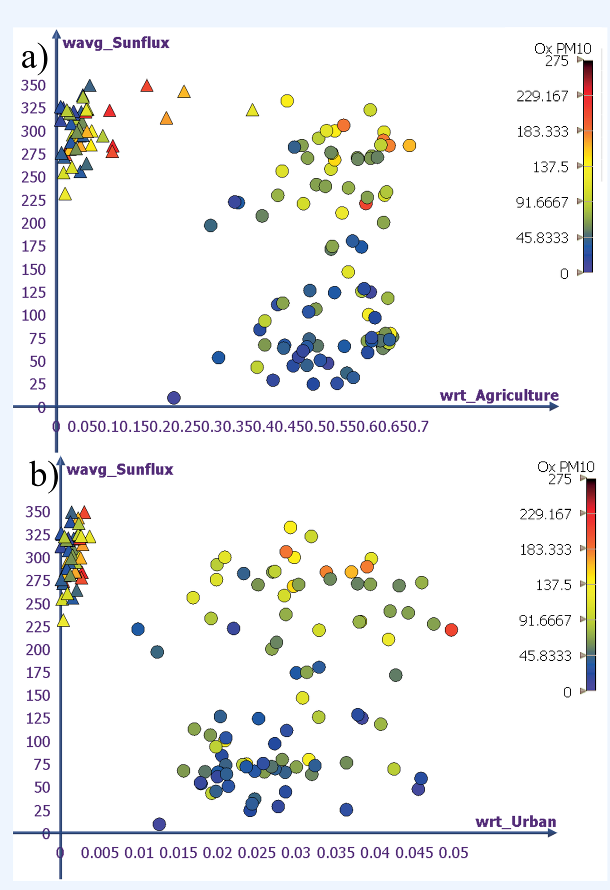

Fig. 12: PM_{10} oxalic acid concentration (in ng m^{-3}) vs. sunflux along trajectory and a) WRT above agricultural areas and b) WRT above urban areas

Principal component analysis (PCA)

Continental sites

- PCA with Varimax rotation identifies two main factors for oxalate at continental sites:
  - **photochemistry**: highest impact on small and large particles
  - **anthropogenic emissions**: highest impact on accumulation mode particles with longest lifetimes in atmosphere

Table 2: Main factors of PCA on cont. dataset with explained variance and factor loadings

	D1	D2	D3	D4
Variance (%)	33.776	17.532	13.195	9.897
Cumulative (%)	33.776	51.308	64.502	74.399
	D1	D2	D3	D4
wrt_agriculture	0.038	**0.900**	0.009	-0.114
wrt_urban	0.126	**0.695**	**0.590**	0.076
wrt_vegetation	-0.101	0.032	**-0.812**	-0.090
avg_trajlength	-0.247	**-0.637**	0.318	0.413
wavg_rainfall	-0.056	-0.140	0.064	**0.847**
wavg_sunflux	**0.800**	0.013	0.330	-0.313
t0_mixdepth	**0.508**	-0.126	0.449	-0.381
Ox 0.05-0.14	**0.840**	0.006	0.015	-0.102
Ox 0.14-0.42	**0.823**	0.170	-0.074	-0.032
Ox 0.42-1.2	**0.521**	**0.529**	-0.348	0.124
Ox 1.2-3.5	**0.830**	0.183	-0.055	0.013
Ox 3.5-10	**0.848**	0.158	0.176	0.046

Coastal site

- Additional factor with high oxalate conc. loadings and no correlation with meteorology or weighted residence times might indicate marine source of oxalic acid (Table 3)

Table 3: Main factors of PCA on coastal dataset with expl. variance and factor loadings

	D1	D2	D4	D3
Variance (%)	34.683	22.279	12.409	12.009
Cumulative (%)	34.683	56.962	69.371	81.380
	D1	D2	D3	D4
wrt_agriculture	**0.903**	0.033	0.023	0.119
wrt_urban	**0.896**	0.157	0.083	-0.058
wrt_vegetation	**0.918**	0.242	0.092	-0.007
avg_trajlength	-0.238	-0.113	**0.758**	0.320
wavg_rainfall	0.186	-0.162	0.024	**0.887**
wavg_sunflux	0.376	-0.114	**0.795**	-0.126
t0_mixdepth	**-0.570**	-0.291	0.354	**0.525**
Ox 0.05-0.14	**0.777**	0.352	-0.113	0.026
Ox 0.14-0.42	**0.584**	**0.652**	-0.214	-0.129
Ox 0.42-1.2	0.363	**0.764**	-0.147	-0.359
Ox 1.2-3.5	0.262	**0.788**	-0.111	-0.360
Ox 3.5-10	-0.004	**0.836**	0.000	0.127

References

- Draxler, R.R. and Rolph, G.D., 2010. HYSPLIT Model PC version 4.9. NOAA Air Resources Laboratory, Silver Spring, MD
- Ervens, B., C. George, J. E. Williams, G. V. Buxton, G. A. Salmon, M. Bydder, F. Wilkinson, F. Dentener, P. Mirabel, R. Wolke, and H. Herrmann (2003), *J. Geophys. Res. [Atmos.]*, *108*(D14), Art. No. 4426
- GLC2000 database, European Commision Joint Research Centre. http://www-gem.jrc.it/glc2000
- Lim, H. J., A. G. Carlton, and B. J. Turpin (2005), *Environ. Sci. Technol.*, *39*(12), 4441-4446
- Neusüß, C., M. Pelzing, A. Plewka, and H. Herrmann (2000), *J. Geophys. Res. [Atmos.]*, *105*(D4), 4513-4527.
- Saxena, P., and L. M. Hildemann (1996), *J. Atmos. Chem.*, *24*(1), 57-109.
- Warneck, P. (2003), *Atmos. Environ.*, *37*, 2423-2427

Leibniz Gemeinschaft